ESR spectroscopy of solid state and biological systems

Arnav Sharma

LS 102-08

Introduction to College Research in Physics

Prof. Doros Petasis

Summer 2022

ALLEGHENY COLLEGE

Abstract

Electron Spin Resonance (ESR) Spectroscopy is a powerful tool that helps in understanding the nature of a biological molecule or a solid-state system. It helps in determining the hyperfine structures, isotropic/anisotropic structure, and resonant magnetic fields. In the present work, this versatile tool was used to determine the g-factor and linewidth of 2,2-diphenyl-1-picrylhydrazyl (DPPH), a biological molecule and the g-factor and hyperfine constant for the solidified solution of $MnCl_2$, a solid-state system. The sample of DPPH sample was kept at room temperature, which is roughly 298 K while the solution of $MnCl_2$ was kept at 104 K . The ESR spectrums were observed and recorded and later analysed to determine the field values and g-factor and line width or hyperfine constant. Finally, a discussion about potential sources of errors in the readings and methodology to reduce them is included.

Introduction

This work aims to analyze the electron spin resonance of a sample of 2,2-diphenyl-1-picrylhydrazyl (DPPH) and a solution of manganese (II) chloride ($MnCl_2$). DPPH is an assay that is widely used to evaluate the properties of plant constituents for scavenging free radicals. From its structure, it can be deciphered to be an organic nitrogen biomolecule molecule. [1] Solidified $MnCl_2$ solution, on the other hand, is a solid-state system.

The g-factor is a dimensionless quantity that provides the information about the magnetic moment and angular momentum of a particle or nucleus. In this paper, more specifically, the g-factor of the electron and nucleus of the samples would be explored. [2] It is used to calculate the gyromagnetic ratio of a sample which is the ratio of a magnetic moment to the angular momentum of a spinning charged particle. [3]

The DPPH sample was chosen due to its chemical nature. It is a free radical with only one unpaired electron and negligible orbital magnetic moment as it moves on a highly delocalized orbit. Due to both these factors, it can be concluded that only the spin of the electron is contributing to the g-factor of DPPH. Hence, the g-factor of DPPH would be close to that of a free electron. [4]

The $MnCl_2$ sample was chosen to expand the scope of this research paper to study the hyperfine structure found from certain samples in an ESR. The hyperfine structure is a result of the interaction between the magnetic field from electron movement and nuclear spin. [5]

Background Theory

Electron Spin Resonance Spectroscopy (ESR also called EPR)

ESR is a form of magnetic resonance spectroscopy that is used to detect transitions induced by electromagnetic radiations between energy levels of electron spins in the presence of an external magnetic field. [6] On doing so, it is possible to determine the g-factor of said particle, which gives further details, such as magnetic moment and angular spin momentum, about the sample.

The ESR spectroscopy relies on the spin of an electron and its associated magnetic moment. When an electron is placed in an external field, $\bar{B}$, it exists in two spin states $m_s = \pm {}^1/_2$. Each spin state corresponds to a different energy level. The lower energy state occurs when the magnetic moment of the electron aligns with the external field, while the higher energy state

occurs when the moment aligns against the external field. This energy difference is a result of the Zeeman effect. [7] Since these are discrete energy states, when microwave radiation of the same energy difference is incident on the sample, the electron will jump from the ground state to an excited state. When this scenario happens, there is resonance. In ESR, this microwave radiation is kept constant; however, the value of the external field varies. At a specific external magnetic field, the condition of resonance, *i.e.*, energy of microwave radiation = energy difference of Zeeman effect is met. At this specific magnetic field, a signal is seen.

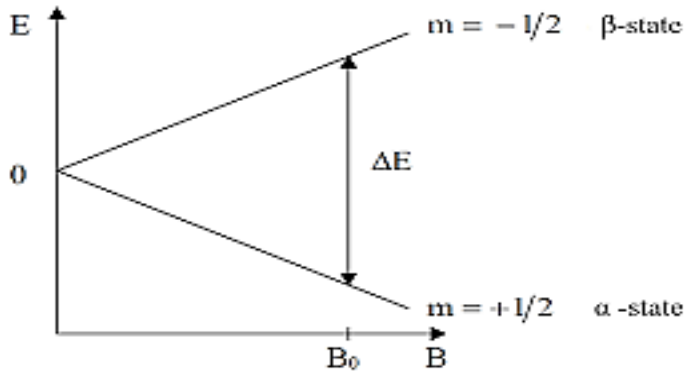

Figure 1.1- Representation of the Zeeman Effect. [8]

In Figure 1.1, it is seen that in the absence of external magnetic field, there is no energy difference between spin states. However, when the magnitude of external magnetic field increases, the energy difference between the spin states increases. Here, $m = -{}^{1}/_{2}$ corresponds to the antiparallel spin state (moment aligning against external field), while $m = {}^{1}/_{2}$ corresponds to the parallel spin state (moment aligning with the external field). At B_0, the energy of microwave radiation would be equal to the energy difference between the spin states, hence a signal would be seen on the ESR.

Derivation for g-factor

The energy of the microwave radiation is given by the equation:

$$E = h\upsilon$$

where h is the Plank's constant and υ is the frequency of microwave radiation. The energy of the magnetic moment of an electron placed in an external magnetic field is given by:

$$E = -\bar{\mu} \,.\, \bar{B}$$

where $\bar{\mu}$ is the magnetic moment of an electron and $\bar{B}$ is the external magnetic field.

According to quantum mechanics, the magnitude of spin angular momentum of an electron is given by:

$$|\bar{S}| = \sqrt{s(s+1)}\,\frac{h}{2\pi}$$

where s is the spin quantum number and h is the plank's constant. For a single electron,

$$|\bar{S}| = \sqrt{\frac{1}{2}\left(\frac{1}{2}+1\right)}\,\frac{h}{2\pi} = \frac{\sqrt{3}}{2}\frac{h}{2\pi}$$

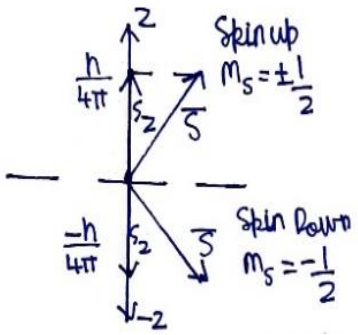

Figure 1.2- Total spin angular momentum along z component

In Figure 1.2, the spin angular momentum is resolved along the z axis with $S_z = Scos\theta = m_s \frac{h}{2\pi}$, where m_s is the spin orientation. m_s can only take 2 values, $m_s = \pm 1/2$. This is seen in Figure 1.2.

The magnetic moment of an electron due to its spin is given by:

$$\overline{\mu_s} = -\frac{e}{m}\bar{S} = -g_e \frac{\mu_B}{\frac{h}{2\pi}}\bar{S}$$

where μ_B is the Bohr magneton and g_e is the g-factor of an electron. [9]

The energy interaction between $\overline{\mu_s}$ and the external field $\bar{B}$ is given by:

$$E = g_e \frac{\mu_B}{\frac{h}{2\pi}} \bar{S}.\bar{\bar{B}} = m_s g_e \mu_B B$$

The difference between energy spin states can be derived as:

$$\Delta E = \frac{1}{2} g_e \mu_B B - \left(-\frac{1}{2} g_e \mu_B B\right) = g_e \mu_B B$$

When resonance is achieved, energy difference between spin states is equal to energy of microwave radiation as shown below:

$$h\upsilon = g_e \mu_B B$$

The g-factor of the electron can thus be experimentally calculated by the formula:

$$g_e = \frac{h\upsilon}{\mu_B B}$$

Substituting the values, we get $g_e = 0.71449 \frac{\upsilon}{B}$, where υ is in GHz and B is in kG.

Hyperfine Lines

The earlier description of the ESR only pertains to compounds without any nuclear spin. However, there are certain compounds that do have a nuclear spin, due to which the nucleus also has a magnetic moment that interacts with the electron moment. Subsequently, the number of signals detected by the ESR spectrometer increases, since even the nucleus spin causes further electron spin splitting due to the coupling of spins. These new signals thus result in

hyperfine lines. The number of these hyperfine lines is given by $2I + 1$, where I is the magnetic nucleus quantum number. [10]

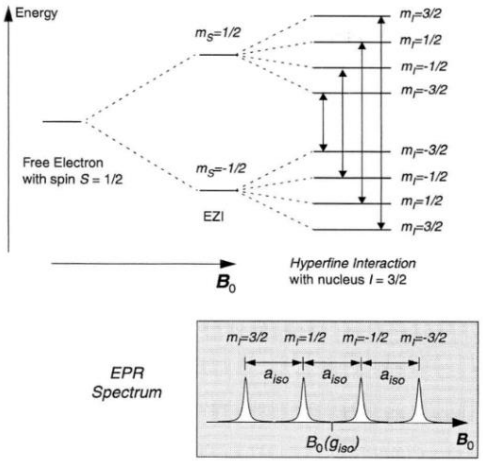

Figure 1.3- Hyperfine lines in ESR [11]

In Figure 1.3, the magnetic nucleus quantum number $I = {}^{3}/_{2}$. Hence, the total number of hyperfine lines seen on the ESR are 4. These four transitions in spin states are shown by the peaks in the ESR spectrum. The change in $m_s = \pm 1$ caused due to the microwave radiation. The a_{iso} is called the Hyperfine constant, and is the measure of the distance between peaks in a spectrum. The magnitude of the hyperfine constant indicates the extent of delocalization of the unpaired electron over the molecule. [11,12]

Experimental Procedure

For both samples, a Varian E-3 X-band EPR spectrometer was used. The only difference between the two samples was the temperature at which the ESP spectroscopy was performed. For the DPPH sample, the spectroscopy was performed at room temperature, while for the $MnCl_2$ the spectroscopy was performed at 104K.

DPPH radical: The following steps describe the experimental methodology:

1. Turn on the coolant water under the fume hood. The coolant water ensures that the magnet does not overheat. The temperature of the ESR should be around room temperature which is 298 K.
2. Set the frequency channel to channel number 3 to get an accurate reading and the intensity of the oscilloscope to all the way to the right and wait for a signal to be seen.
3. When the signal is seen, place the sample in the cavity. There should be a dip displayed on the oscilloscope. Set the mode to tune and adjust the position of the horizontal dip until it reaches the blackline by utilizing the frequency knob. Bottom out the dip by rotating the Teflon rod located behind the cavity.
4. Once the dip is in a proper position, the mode knob can be turned to operate, and the recorder switch can be turned on. The frequency and power attenuation knobs should be adjusted to ensure the frequency error and detector are in proper positions.
5. The magnetic field mid-range and scan range can be set, and the scan button can be pushed to start the room temperature EPR run. [13]

***$MnCl_2$ solution*:** The procedure for the solution of $MnCl_2$ solution sample is similar to that of DPPH; however, the difference lies in the temperature. Here we intend to freeze the solution into a solid, hence a low temperature of 104 K would be required. When conducting a low temperature EPR run, the temperature cooler needs to be turned on after coolant water is turned on. The main valve of the nitrogen tank should be opened, and the liquid nitrogen should flow with a pressure around 25 to 30 psi. Once liquid nitrogen is in the dewar, the sample needs to be slowly lowered into it. Going slowly is essential as otherwise the EPR tube will break. Once the sample is cooled, it can be placed in the cavity. The steps now for the EPR are same as for the room temperature sample. [13]

The following image demonstrates the features of an EPR and Table 2.1 details parts of the EPR along with a short description and methodology during the experiment.

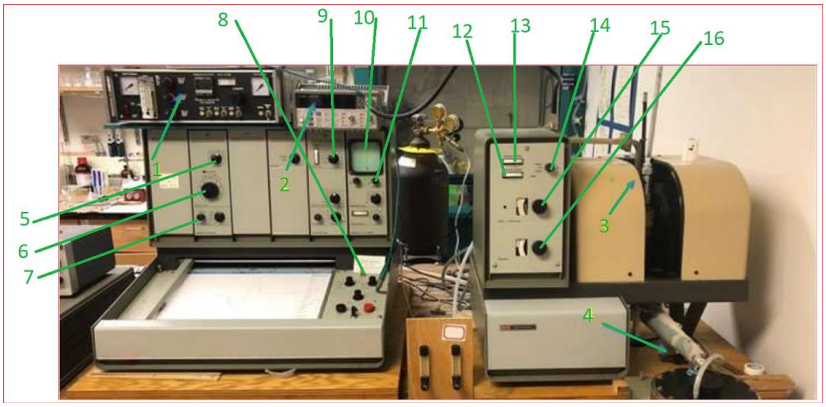

Figure 2.1- An ESR set up [13]

Table 2.1- Components of ESR [13]

Sr no.	Feature	Description
1	Temperature controller	Monitor temperature and nitrogen flow for samples at low temperature
2	Universal Counter	Displays frequency of MW
3	Cavity	Sample placed here
4	Dewar	Liquid Nitrogen to cool the sample
5	Thousands Control	Incremental increase of magnetic field to 1 kG
6	Vernier Dial	Set field increments from 0 to 1000G
7	Scan range	
8	Recorder Switch	Switched on to plot the signal during the experiment
9	Receiver Gain	Controls intensity of received of signal
10	Oscilloscope	Helps in Tuning the instrument
11	Intensity Knob	Manipulates intensity of signal on the oscilloscope. Turned all the way to the right
12	Detector Current	Must be kept in the green region
13	Frequency Error	Must be positioned at 0
14	Mode Knob	Set to tune while tuning the spectroscope. Set to operate while running the experiment
15	Power Attenuation knob	Controls amount of microwave radiation entering the cavity. It is turned to ensure detector current in green region
16	Frequency knob	It is turned in order to ensure frequency error reaches 0. It ensures klystron frequency is equal to resonance frequency

Results and Discussion

DPPH radical-

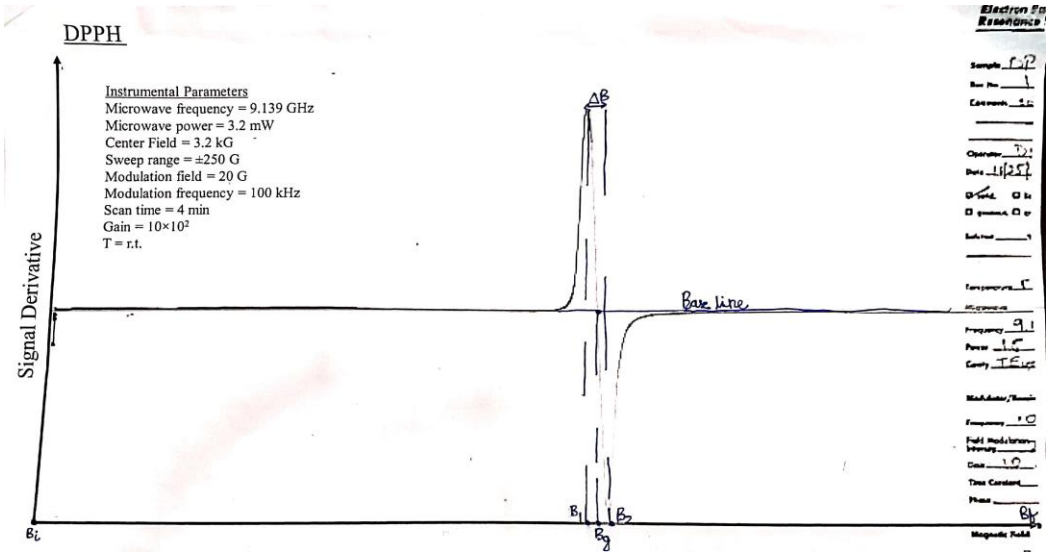

Figure 3.1- ESR spectrum of DPPH

Given the central field is $3.20\ kG$, and the sweep range is $\pm 0.250\ kG$, we can determine the initial and final magnetic field. $B_i = 3.20 - 0.250 = 2.95\ kG$. $B_f = 3.2 + 0.25 = 3.45\ kG$

The length of the spectrum $w_s = 28.0cm$

The field range $= 3.45 - 2.95 = 0.50\ kG$

On scaling the spectrum, we get $1cm = \frac{0.50}{28} = 0.0179\ kG$

Table 3.1 summarizes the results of ESR of DPPH.

Table 3.1- DPPH ESR

Field	Distance from B_i ($cm\ with\ uncertainty\ \pm 0.1cm$)	Field Strength ($kG\ with\ uncertainty \pm 0.00179kG$)
B_1	15.4	3.226
B_g	15.6	3.229
B_2	15.9	3.235

The g factor of DPPH is given by $g_e = 0.71449\frac{\upsilon}{B}$.

The resonance field $= B_g = 3.23\ kG$ and frequency$= \upsilon = 9.139\ GHz$

$$g_e = 0.71449 \times \frac{9.139}{3.229} = 2.022$$

$$\Delta g_e = \frac{\Delta B_g}{B_g} \times g_e = 0.001121$$

$$g_e = 2.022 \pm 0.001121$$

The theoretical value of the g-factor of a DPPH sample is 2.00. [14]

The percent error in our calculated g-factor $= \frac{2.022-2.00}{2.00} \times 100 = 1.1\%$.

This value of g-factor is acceptable because it lies within the range of experimental accuracy.

The linewidth is given by $\Delta B = B_2 - B_1 = 0.009kG \pm 0.00358\ kG = 9G \pm 3.58G$

The literature linewidth is $4.7G$. [15]

The percent error in our linewidth $= \frac{9-4.7}{4.7} \times 100 = 91.5\%$.

This high percent error can be attributed to the large uncertainty and systematic error. Methods to reduce error and uncertainty in the linewidth is given at the end of the discussion.

We have experimentally shown that the g-factor of DPPH is close to 2.00, the g-factor of a free electron. This indicates that it is a free radical since an unpaired electron has very little orbital contribution to the magnetic moment. Moreover, the signal is an isotropic spectrum, which implies symmetry is produced by all other atoms in the lattice at the location of the paramagnetic ion. [16]

$MnCl_2$ solution-

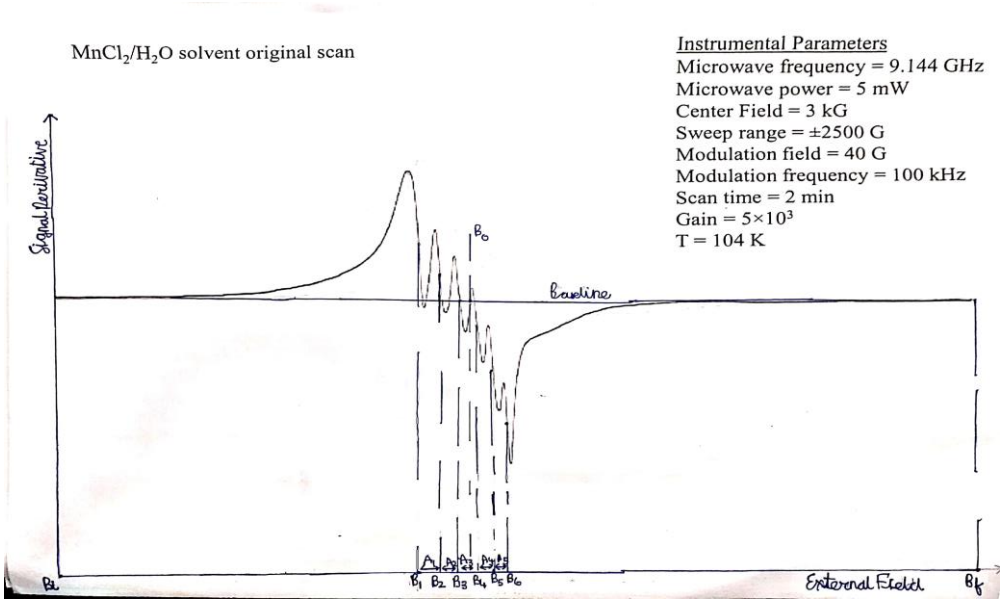

Figure 3.2- ESR spectrum of $MnCl_2$ solution

Given the central field is $3.00\ kG$, and the sweep range is $\pm 2.50\ kG$, we can determine the initial and final magnetic field. $B_i = 3.00 - 2.50 = 0.50\ kG$. $B_f = 3.00 + 2.50 = 5.50\ kG$

The length of the spectrum $w_s = 27.0cm$

The field range $= 5.50 - 0.50 = 5.00\ kG$

On scaling the spectrum, we get $1cm = \frac{5.00}{27} = 0.185\ kG$

The formula to calculate the field strength at distance d is given by:

$$B = B_i + \left(\frac{B_f - B_i}{w_s}\right) d$$

$$B = 0.50 + 0.185d$$

The g-factor is given by $g_e = 0.71449 \times \frac{9.144}{B_n}$, where B_n is the resonant field and 9.144 is the frequency of microwave radiation in GHz

The uncertainty in g-factor is given by $\Delta g_e = \frac{0.0185}{B_n} \times g_e$, where 0.0185 is the uncertainty in resonance field in kG.

Table 3.2 summarizes the results of the $MnCl_2$ Solution

Table 3.2 $MnCl_2$ Solution ESR

Field	Distance from B_i (cm *with uncertainty* $\pm 0.1cm$)	Field Strength (kG *with uncertainty* $\pm 0.0185kG$)	g-factor	Uncertainty in g-factor
B_1	10.7	2.48	2.63	0.0197
B_2	11.3	2.59	2.52	0.0180
B_3	11.8	2.68	2.44	0.0168
B_0	12.1	2.74	2.39	0.0161
B_4	12.4	2.79	2.34	0.0155
B_5	12.9	2.89	2.26	0.0145
B_6	13.3	2.96	2.21	0.0138

The average g-factor is given by $g_{avg} = \frac{\sum_{i=1}^{6} g_i}{6} = 2.40 \pm 0.0164$. Note: the calculation of the average g-factor does not use the field strength B_0.

The magnetic field at the centre of the hyperfine spectrum is B_0 with g-factor $g_0 = 2.39 \pm 0.0161$. B_0 was chosen as the centre of the hyperfine spectrum because the spectrum was almost symmetric at this point. Calculating percent difference between g_{avg} and g_0 with respect to g_{avg}. Percent difference $= 0.417\%$. The percent difference is small, however, it can be further reduced.

In this paper, we would be considering g_0 to be the experimental g-factor of the $MnCl_2$ Solution.

The literary g-factor for $MnCl_2$ solution at $104K$ is $g_0 = 2.00$ [17]

Percent error $= \frac{2.44-2.00}{2.00} \times 100 = 22.0\%$

The percent error in the experimental value is significant. This can be due to the fact that the electrons of the manganese (II) ions still being bound due to the frozen water of crystallization and due to experimental error. The suggestions to reduce the experimental error are given at the end of the discussion.

Table 3.3- Hyperfine Constant Values of $MnCl_2$ solution

Hyperfine Constant	Hyperfine constant value (kG $with$ $uncertainty$ $\pm 0.0370 kG$)
$A_1 = B_2 - B_1$	0.11
$A_2 = B_3 - B_2$	0.09
$A_3 = B_4 - B_3$	0.11
$A_4 = B_5 - B_4$	0.10
$A_5 = B_6 - B_5$	0.07

The average hyperfine constant $A = 0.096\ kG \pm 0.0370 kG = 96G \pm 37G$

The expected hyperfine constant according to library sources is $90G$ [17]

The percent error in the hyperfine constant is 6.67%.

Although, the hyperfine constant lies within the range of the experimental accuracy, the error can still be reduced. Furthermore, the large uncertainty can also be minimized.

The ESR spectrum of the $MnCl_2$ solution has also shown 6 hyperfine lines. From this, we can deduce the magnetic nuclear quantum number $I = {}^{5}/_{2}$. The g-factor of $MnCl_2$ solution suggests the electron was bound to the atom as the g-factor was greater than the free electron, whereas in theory it should be a delocalized electron. This result can be caused due to the frozen water of crystallization that prevents the electron from becoming delocalized.

It is possible to increase the accuracy of determining the g-factor of $MnCl_2$ solution and the linewidth of the DPPH radical. Although the hyperfine constant of the $MnCl_2$ solution and the g-factor of the DPPH radical were in limits of experimental accuracy, it is still plausible to achieve a higher accuracy and precision.

The major limitation in all experimental readings was determining the resonant field and other key field lines by hand. This resulted in the error between the experimental values and the literature values for both samples. Furthermore, by using hand analysis, the uncertainty in the field strengths also increased, which skewed the readings. To avoid these errors, a computer generated and well resolved image of the ESR spectrum can be used. To reduce systematic errors, there should be a special alignment procedure for accurate sample positioning within the microwave cavity. Furthermore, a double TE_{104} rectangular cavity should be used. [18] These methods can improve the precision and accuracy for all the experimental readings.

The linewidth of the DPPH sample and the g-factor of the $MnCl_2$ solution had shown high experiment percentage error. It is though possible to increase the accuracy of these readings. To increase the accuracy in determining the linewidth of the DPPH sample, the modulation field can be lowered to have a sharper signal. On doing so, it becomes relatively simpler to measure the distance between the peaks of the signal derivative. To reduce the error in the g-factor of the $MnCl_2$ solution, the sweep range and width should be reduced. By having a larger field range, the uncertainty in g-factor increases, and the precision of the plotter decreases, causing a faulty value in the g-factor. On using a lower sweep width, the precision and accuracy of the plotter should increase, and we would see broader spectrums. The broader spectrum helps reduce the uncertainty in the measurement of the g-factor and attain a more accurate

value. By employing all these techniques, the percent uncertainty and error in linewidth of the DPPH sample and g-factor of the $MnCl_2$ solution would fall.

Conclusion

Overall, it is interesting to note the difference between the solid-state system $MnCl_2$ solution and the biological system DPPH. The most significant difference between these systems was the hyperfine structure in the $MnCl_2$ solution, which was not present in the DPPH sample. The relatively high magnetic nuclear quantum number $I = {}^{5}/_{2}$ of the $MnCl_2$ solution is also intriguing. Another major difference between the DPPH sample and the $MnCl_2$ solution was the g-factor. DPPH had the experimental g-factor of 2.02, which is significantly lower than the $MnCl_2$ solution's experimental g-factor of 2.40. The large difference in the g-factor could be accounted for as the electron of the manganese (II) chloride ion still being bound to the sample, due to the frozen water of crystallization. This in turn affects the g-factor of the sample. It is probable that this is a property of other solid-state systems as well. However, it should also be noted that the experimental g-factor of the $MnCl_2$ solution had a high percentage error.

In conclusion, ESR has enabled to understand the atomic and subatomic properties of biological and solid-state systems. In the future, more investigations can be done that search for a corelation between g-factors and a physical parameter. For instance, in context of biological systems, there is scope of research in investigating the impact of temperature on the g-factor of DPPH or any other biomolecule. On the other hand, with respect to solid-state systems, there can be an investigation that relates the g-factor with the amount of water of crystallization in the sample.

References

1. K. Pyrzynska and A. Pękal, "Application of free radical diphenylpicrylhydrazyl (DPPH) to estimate the antioxidant capacity of food samples," Analytical Methods, vol. 5, no. 17, p. 4288, 2013.
2. "G-Factor (physics)," DBpedia. [Online]. Available: https://dbpedia.org/page/G-factor_(physics). [Accessed: 05-Aug-2022].
3. D. Bowen, "The real reason why the electron's Bare g-Factor is 2 times classical," Journal of Modern Physics, vol. 07, no. 10, pp. 1200–1209, 2016.
4. R. Palai, "Electron Spin Resonance: An Experiment for Perceiving Quantum Physics Intuition." [Online]. Available: https://advlabs.aapt.org/bfyii/files/RPalai_AAPT2015.pdf. [Accessed: 05-Aug-2022].
5. Libretexts, "Hyperfine structure," Chemistry LibreTexts, 15-Aug-2021. [Online]. Available: https://chem.libretexts.org/Bookshelves/Physical_and_Theoretical_Chemistry_Textbook_Maps/Supplemental_Modules_(Physical_and_Theoretical_Chemistry)/Quantum_Mechanics/13%3A_Fine_and_Hyperfine_Structure/Hyperfine_Structure. [Accessed: 05-Aug-2022].
6. R. Miglani, "ESR full form: Definition, principle & advantages! ." [Online]. Available: https://byjusexamprep.com/esr-full-form-i. [Accessed: 04-Oct-2021].
7. "What is EPR?," The University of Texas at Austin EPR facility . [Online]. Available: https://sites.cns.utexas.edu/epr_facility/what-epr. [Accessed: 05-Aug-2022].

8. “A52 basics of NMR (the nuclear zeeman E ECT) - ipc.kit.edu.” [Online]. Available: https://www.ipc.kit.edu/english/1925.php. [Accessed: 05-Aug-2022].
9. Libretexts, “EPR - theory,” Chemistry LibreTexts, 16-Apr-2022. [Online]. Available: https://chem.libretexts.org/Bookshelves/Physical_and_Theoretical_Chemistry_Textbook_Maps/Supplemental_Modules_(Physical_and_Theoretical_Chemistry)/Spectroscopy/Magnetic_Resonance_Spectroscopies/Electron_Paramagnetic_Resonance/EPR_-_Theory. [Accessed: 05-Aug-2022].
10. L. Zhuang and J. Lu, “Chapter 13 - In-situ ESR for Studies of Paramagnetic Species on Electrode Surfaces and Electron Spins Inside Electrode Materials,” in Dian Hua Xue Xi Fu he Dian Cui Hua de Yuan Wei Guang Pu Yan Jiu: Dao Du Ban = in-situ spectroscopic studies of adsorption at the electrode and electrocatalysis, Beijing: Ke xue chu ban she, 2008, pp. 409–410.
11. “Hyperfine interaction,” Electron Paramagnetic Resonance . [Online]. Available: https://epr.ethz.ch/education/basic-concepts-of-epr/int--with-nucl--spins/hyperfine-interaction.html. [Accessed: 05-Aug-2022].
12. Libretexts, “Hyperfine splitting,” Chemistry LibreTexts, 16-Apr-2022. [Online]. Available: https://chem.libretexts.org/Bookshelves/Physical_and_Theoretical_Chemistry_Textbook_Maps/Supplemental_Modules_(Physical_and_Theoretical_Chemistry)/Spectroscopy/Magnetic_Resonance_Spectroscopies/Electron_Paramagnetic_Resonance/Hyperfine_Splitting#:~:text=The%20hyperfine%20coupling%20constant%20(a,constant%20may%20also%20be%20calculated. [Accessed: 05-Aug-2022].
13. D. Petasis, “Varian E-3 X-band EPR Spectrometer.” .
14. U. G. Ahmad, S. Shukur, and A. I. Ridwan, “Study and Determination of Lande g-Factor of DPPH-Diphenyl Picryl Hydrazyl using Electron Spin Resonance Spectrometer,” *IJESC*, vol. 6, no. 4, pp. 3814–3814.
15. C. P. Poole, “*Sensitivity* ,” in Electron spin resonance: A comprehensive treatise on experimental techniques, New York: Dover Publications, 1996, pp. 443–443.
16. D. Petasis, “EPR Handout 1.”
17. D. Petasis, “Lecture ESR-07.” .
18. M. Mazur, “A dozen useful tips on how to minimise the influence of sources of error in quantitative electron paramagnetic resonance (EPR) spectroscopy—a review,” *Analytica Chimica Acta*, vol. 561, no. 1-2, pp. 1–15, 2006.